

Parameter Uncertainties for a 10-Meter Ground-Based Optical Reception Station

K. Shaik

Communications Systems Research Section

Performance uncertainties for a 10-m optical reception station may arise from the nature of the communications channel or from a specific technology choice. Both types of uncertainties are described in this article to develop an understanding of the limitations imposed by them and to provide a rational basis for making technical decisions. The performance at night will be considerably higher than for daytime reception.

I. Introduction

A 10-m hexagonally segmented Cassegrain optical telescope has been proposed for use as an Earth-based receiver for laser communications from planetary spacecraft [1-4]. Such a reception station on the ground may provide, for example, a nighttime channel capacity of about 300 kb/sec for a 0.5-m-diameter transmitter using a 2-W frequency-doubled Nd:YAG laser at Saturn. While the first reception station will be ground based, the goal is to develop and demonstrate the technology to put a telescope in Earth's orbit, where it can avoid the deleterious effects of the atmosphere on optical communications. For this reason, the technology has to be economical enough to allow replication for either a ground- or a space-based network.

The deep-space optical reception antenna (DSORA) will be designed to allow direct detection of optical signals for typical data rates from planetary spacecraft despite the presence of considerable solar background interference. It will also have the ability to acquire and navigationally

track spacecraft signals relative to the stellar background by a two-telescope system described earlier [5].

This article presents a study of the performance uncertainties for the DSORA. Some of the uncertainties are technology dependent and will become smaller once a specific technology choice has been made, while others arise from inherent random fluctuations in the transmission channel. To design a viable system, one must understand these fluctuations' ultimate effect on optical communications.

II. Parameter Uncertainty Analysis

To quantify these parameter uncertainties, calculations were made for a typical Earth-Saturn optical communications link using a computer program described in [6]. Table 1 provides a list of transmitter characteristics and other operational parameters used in the link calculation. Table 2 enumerates the DSORA parameters along with

their base value and range of meaningful parameter uncertainties. For example, the blur circle size for the system may range from 184 to about 28 μrad . However, the nominal or base value of 162 μrad represents the best estimate of blur circle size now being derived from the type of technology being considered for DSORA. The last two columns in Table 2 show the upper and lower bounds of the link margin in dB for each parameter when all other parameters are held at their base value. However, daytime background and stray-light irradiance are treated as one parameter and are varied together to obtain favorable and adverse link margins. The reason for doing this is discussed later.

Figure 1 shows the results graphically. It shows a baseline link margin of 3.0 dB, when only the base values for the design parameters are used in the link calculations. The range of uncertainty for each of the parameters is shown by vertical lines on the graph. Each of these parameter uncertainties will be discussed below; however, atmospheric transmission, sky background and stray-light irradiance, and blur circle size will be considered in greater detail since they represent the largest range of uncertainty for DSORA and because it will be cost-effective to attempt to reduce their effect on system performance.

For a ground-based DSORA, the atmospheric transmission loss and background noise from sky irradiance are inherent to the communications channel and arise as light travels through the Earth's atmosphere. Sections II.A and II.B provide a detailed analysis of these uncertainties. Section II.C studies the telescope's blur circle size, a large source of uncertainty which almost entirely depends on the choice of technology. Section II.D considers the other performance uncertainties identified in Table 2.

A. Atmospheric Transmission

Development of robust line-of-sight Earth-space optical communications depends on an accurate description of the expected propagation loss through the atmosphere. In the absence of thick clouds that can completely close down a communications link, the transmission loss is primarily due to absorption and scattering by molecules, aerosols, fog, haze, and other particulate matter in the atmosphere. Table 2 shows a range (from favorable to adverse) of atmospheric transmittance for a wavelength corresponding to a frequency-doubled Nd:YAG laser (0.532 μm) transmitter.

One of the most complete compilations of molecular absorption data was developed at the Air Force Geophysics Laboratory (AFGL). The High Resolution Transmission (HITRAN) database in conjunction with the computer

program FASCOD (Fast Atmospheric Signature Code) [7,8] gives various parameters for almost 350,000 lines over a spectral region from ultraviolet to millimeter waves with a resolution of 10^{-5} cm^{-1} . This code can be used to make a detailed study of laser frequencies that are likely to be used for communications purposes and ensures that the carrier frequency does not fall on a strong absorption line. Once this is accomplished—by tuning the transmitter laser away from strong absorption lines—the computer code LOWTRAN (Low Resolution Transmission), also developed by AFGL, can be used to obtain averaged signal attenuation for an atmosphere characterized by fog, haze, cirrus clouds, and other particulate matter [9]. LOWTRAN also has the ability to compute sky irradiance, as seen in the next section.

The data results of the investigation using LOWTRAN7 (Version 7 of LOWTRAN) are shown in compact graphic form in Fig. 2. The calculations have been made with a slanted ground-to-space path for a zenith angle of 45 deg. Since the station is likely to be placed on a mountaintop to reduce transmission loss, a ground altitude of 2 km corresponding to the Table Mountain Observatory (TMO) has been chosen for the calculations. The U.S. Standard Atmosphere, as well as the presence of standard cirrus clouds, has been assumed. As defined by the International Radio Consultative Committee (CCIR), a visibility of 23.5 km represents "standard clear" conditions. The transmission efficiency at this visibility is 0.48, and this is used as the base value for the atmospheric transmission for DSORA. Visibilities greater than 35 and less than 4 km are rare and, as such, the atmospheric transmittances at these visibilities are chosen to represent favorable and adverse limits for the station. Note that the reception station is not expected to operate under cloudy conditions, which may happen 40 percent of the time in the southwestern U.S.

The results presented here are site independent and use generalized atmospheric models to quantify transmittance at optical frequencies for an Earth-space path. These results should help in the process of site selection for the DSORA. Once a site for the ground station has been selected, a more accurate atmospheric profile for the chosen area can be obtained empirically and used to obtain still better estimates of the link loss due to the atmosphere.

B. Sky Background and Stray-Light Irradiance

Several sets of daytime sky irradiance calculations using LOWTRAN7 software from AFGL have been made. Sample results for sky irradiance at 0.532 μm for a solar zenith angle of 45 deg are shown in Figs. 3-5. All graphs

assume the presence of standard cirrus clouds, using one of the cirrus cloud models as defined by LOWTRAN and the 1976 U.S. Standard Atmosphere.

Figure 3 shows sky irradiance at $0.532\ \mu\text{m}$ as a function of solar elongation when the solar zenith is 45 deg and the observation platform is at a height of 2 km (about the height of TMO). The visibility of the atmosphere is assumed to be 23.5 km, which corresponds to standard clear conditions, as stated earlier. The observation instrument is made to scan the sky along the elevation axis. The solar elongation is considered positive along the direction of increasing zenith angle and is negative otherwise. The results are not symmetric about the Sun as the length of the atmosphere traversed depends on the zenith angle. Figure 4 shows the sky irradiance when it is scanned along the azimuthal direction. As the results are symmetric about the Sun, this plot shows solar elongation on only one side of the Sun. All other parameters are the same as in Fig. 3. Note that for both the graphs the calculations were not made for solar elongations of less than 5 deg. Figure 5 shows the effect of atmospheric visibility on the received sky irradiance for a fixed solar elongation of 10 deg.

To summarize, the LOWTRAN calculations predict that the sky irradiance can be as high as $0.65\ \text{W}/(\text{m}^2\cdot\text{sr}\cdot\text{nm})$ for solar elongations of 10 deg (see Fig. 5). It reduces to a value of about $0.3\ \text{W}/(\text{m}^2\cdot\text{sr}\cdot\text{nm})$ when solar elongation is 30 deg, and then to $0.1\ \text{W}/(\text{m}^2\cdot\text{sr}\cdot\text{nm})$ for solar elongation of about 90 deg. The sky background irradiance at night is on the order of $0.5 \times 10^{-8}\ \text{W}/(\text{m}^2\cdot\text{sr}\cdot\text{nm})$ and does not limit the performance of the optical communication links considered here.

The graphs shown in Figs. 3–5 represent only one set of conditions. Calculations for other solar zeniths and atmospheric conditions can be made by changing the program inputs. The value of sky irradiance at solar elongation of 45 deg is about $0.17\ \text{W}/(\text{m}^2\cdot\text{sr}\cdot\text{nm})$ and is being used as the base value for the system. The values 0.65 and $0.1\ \text{W}/(\text{m}^2\cdot\text{sr}\cdot\text{nm})$ represent the range of uncertainty for daytime sky background irradiance as shown in Table 2.

The calculations and the experimental data show that sky irradiance constitutes a very large source of background radiation for daytime observations. The detected background power can be approximately two or more orders of magnitude higher than the signal power for typical deep-space communication links. A number of precautions will be necessary to recognize the signal in the presence of this kind of background power. Techniques to reduce background interference include highly signal-selective reflection coatings on the mirrors and a sub-angstrom filter

in front of the detector to reject out-of-band radiation. Unlike the signal source, the sky is an extended source of radiation. An effective way to cope with the sky background irradiance will be to reduce the system blur circle size.

Stray light can be an important contributor to background noise for both the Earth-orbiting and ground-based DSORA, especially when the system must operate at small solar elongations. Stray light is light that enters the front end of the DSORA at an oblique angle or an angle larger than the system's field of view (FOV), but after many specular reflections and scattering events finds its way to the detector of interest. This problem has not yet been studied in adequate detail. However, a preliminary estimate, tied to the solar background irradiance for a ground-based system, has been made. The direct sunlight striking the sunshade at the front end of the DSORA with an FOV of about 20 deg will suffer many reflections off baffles and shrouds before it reaches the detector, whose FOV will be less than $200\ \mu\text{rad}$. Since nonoptical surfaces will be coated for a reflectance of less than 0.01, the expected intensity of stray light from direct sunlight reaching the baffle at the detector will be much smaller than the daytime sky background irradiance. The sky background irradiance reaching the detector after being reflected twice off this baffle is assumed to be the base value for stray-light irradiance. Sky background reflected one and three times off the baffle will be used as the adverse and the favorable limits, respectively. Note that the stray-light irradiance reaching the detector, as defined, will depend on sky background irradiance only. For this reason, the effects of sky background and stray-light irradiance have been computed together in Table 2, and have been shown as one vertical bar in Fig. 1.

C. Blur Circle Size

Blur circle size of the telescope represents a large design uncertainty that is almost entirely due to the choice of technology. The contributing factors to this large blur radius include the surface quality and the gravity sag of the primary mirror; the piston, tilt, and decenter of the mirror segments due to mechanical and thermal effects; and atmospheric and dome seeing conditions. Technical solutions exist to eliminate all sources of error to the point where the size of the blur circle is dominated by atmospheric seeing alone. In fact, this is the case for most astronomical telescopes in use today. Such accuracy for the DSORA is neither required nor desirable in order to keep the cost of the system low. As mentioned in the last section, decreasing the blur circle size will be an effective way to reduce the sky background photon counts without affecting the

signal counts adversely. However, note that system performance improves significantly only when it is limited by the background irradiance from extended sources. For the ground-based DSORA, this will include almost all daytime observations and those long-distance communication links for which nighttime sky irradiance limits the system sensitivity.

Table 3 lists base, favorable, and adverse estimates for the described effects to the blur radius for the present DSORA design. In terms of the root-mean-square (RMS) roughness σ and the correlation distance T of the mirror surface, the expected blur diameter for 80 percent encircled energy in radians is expressed as $11.3 \sigma/T$ [10]. For the present design with $\sigma = 2 \mu\text{m}$ and $T = 0.25 \text{ m}$, the quality of the mirror contributes $90 \mu\text{rad}$. This number is used as the base and adverse value. If σ for the mirror is reduced to $0.5 \mu\text{m}$, which is still quite rough compared to present-day astronomical telescopes, this contribution will become $23 \mu\text{rad}$ (favorable value). The gravity sag for the Keck Telescope without active controls is predicted to be $100 \mu\text{rad}$ and this is the number that is used here for the base as well as the adverse value [11]. Thermal and mechanical force-loading effects for the Keck Telescope and the National Optical Astronomy Observatories' (NOAO) 8-m telescope design without active controls was expected to be about $30 \mu\text{rad}$. Since DSORA is expected to operate during the daytime at small solar elongations, the thermal forces will be three to four times higher. The base value for the thermal and mechanical error is obtained by escalating $30 \mu\text{rad}$ by a factor of 3, while the adverse value uses a factor of 4. Possible use of active controls can reduce the errors due to gravity sag and thermal forces to small residual levels, depending on the bandwidth of the control system. Small values of $10 \mu\text{rad}$ for each of the two parameters are used in the favorable column. Note that it is the mirror quality that will dominate the total RMS blur diameter in the column for favorable values. The atmospheric and dome seeing errors for most mountaintops are less than $5 \mu\text{rad}$, but may escalate to about $25 \mu\text{rad}$ during midmornings and late afternoons. Active controls that are being considered for the station will have sub-hertz bandwidths and will not help in reducing the contribution to blur diameter due to relatively fast atmospheric phenomena. The rows for atmospheric and dome seeing parameters in Table 3 reflect this observation. The total RMS blur diameter values for base, favorable, and adverse conditions are 162, 28, and $184 \mu\text{rad}$, respectively. These are the values used in Table 2 and shown in Fig. 1.

For a ground-based DSORA limited by sky background irradiance, the system sensitivity or the signal-to-noise ratio (SNR) is proportional to D/ϕ , where D is the diameter

of the telescope and ϕ is the blur circle radius. Therefore, the gain in sensitivity that can be obtained by reducing ϕ by half, for example, is equivalent to what may be achieved by doubling the telescope diameter. Whereas the cost of telescopes historically varies approximately as $D^{2.5}$, the European Southern Observatory (ESO) has estimated¹ that the cost of figuring the primary mirror varies as D . Hence, it may be possible to improve the surface quality of the mirror and to incorporate low-level active controls to reduce the blur circle size. Preliminary estimates show that daytime data rates can be improved by a factor of 3 if the blur circle diameter for the ground-based DSORA can be reduced to $50 \mu\text{rad}$. However, the improvement in data rates will be small for nighttime observations and for the spaceborne DSORA since sky background irradiance is very small in these cases and does not limit system performance.

D. Other Parameters

Other technology-dependent uncertainty parameters include receiver optics efficiency, filter bandwidth and efficiency, and detector efficiency. The range of uncertainty for these parameters is relatively small and has been identified in Table 2 for a typical deep-space optical communications link. The first three columns in Table 2 provide a base and range of possible values (from favorable to adverse) for the listed parameters.

Receiver optics efficiency may vary from 0.4 to 0.7 and essentially depends on surface quality and the type and number of coatings on the optical elements in the optical path. The major trade-off here is between the pass-band and the efficiency of the optical coatings. Generally, the optical coatings with higher passbands have lower efficiencies. A bank of optical filters, including the interference and atomic type, may be employed with the DSORA. Choice of a specific filter will then depend on given channel characteristics. The bandwidth and the efficiency of a filter are generally related to each other; larger bandwidth filters usually provide higher efficiencies. As with optical filters, a set of detectors will also be available for the DSORA and the choice of a given detector (and the detector efficiency) will depend on the channel characteristics. As the DSORA design progresses and appropriate technology choices are made, the foregoing uncertainties – which are already small compared to the ones discussed separately above – will be reduced further.

Note that the uncertainty parameters discussed in earlier sections strongly affect the performance of an Earth-

¹ ESO's Very Large Telescope (VLT) Report No. 44, 1986.

based DSORA. For spaceborne systems, the absence of an atmosphere eliminates both signal transmission loss due to atmosphere and the sky as an extended source of strong background irradiance. It also greatly relieves the pressure to have a small blur diameter to avoid integrating background light over a larger sky area.

III. Conclusion

The data rates expected from DSORA will be determined by the parameters discussed above. Most of these parameter uncertainties, like blur circle size, depend upon

the choice of technology. It will be necessary to continually estimate the cost performance of improving technology to develop an optimal design. Atmospheric transmittance is by far the most random parameter that will affect the day-to-day performance of the system. The choice of an appropriate site and identification of directional pointing to a particular deep-space mission will provide some help in reducing uncertainty in atmospheric transmission. Also, identification of a particular mission will have a dramatic effect on sky background irradiance uncertainty. The performance of DSORA will be considerably higher for missions that use the optical communications channel at night rather than during the day.

References

- [1] E. L. Kerr, "Strawman Optical Reception Development Antenna (SORDA)," *TDA Progress Report 42-93*, vol. January-March 1988, Jet Propulsion Laboratory, Pasadena, CA, pp. 97-110, May 15, 1988.
- [2] E. L. Kerr, "An Integral Sunshade for Optical Reception Antennas," *TDA Progress Report 42-95*, vol. July-September 1988, Jet Propulsion Laboratory, Pasadena, CA, pp. 180-195, November 15, 1988.
- [3] E. L. Kerr, "Architectural Design of a Ground-Based Deep-Space Optical Reception Antenna," submitted for publication in *Opt. Eng.*
- [4] K. S. Shaik and E. L. Kerr, "A Ten-Meter Optical Telescope for Deep Space Communications," *SPIE*, vol. 1236, ed. L.D. Barr, pp. 347-350, February 1990.
- [5] K. S. Shaik, "A Two-Telescope Receiver Design for Deep-Space Optical Communications," *TDA Progress Report 42-101*, January-March 1990, Jet Propulsion Laboratory, Pasadena, CA, pp. 114-120, May 15, 1990.
- [6] W. K. Marshall and B. D. Burk, "Received Optical Power Calculations for Optical Communications Link Performance Analysis," *TDA Progress Report 42-87*, vol. July-September 1986, Jet Propulsion Laboratory, Pasadena, CA, pp. 32-40, November 15, 1986.
- [7] L. S. Rothman, R. R. Gamache, A. Barbe, A. Goldman, J. R. Gillis, L. R. Brown, R. A. Toth, J. M. Flaud, and C. Camy-Peyret, "AFGL Atmospheric Absorption Line Parameters Calculation: 1982 Edition," *Appl. Opt.*, vol. 22, no. 15, pp. 2247-2256, August 1, 1983.
- [8] S. A. Clough, F. X. Kneizys, E. P. Shettle, and G. P. Anderson, "Atmospheric Radiance and Transmittance: FASCOD2-Fast Atmospheric Signature Code," Sixth Conference on Atmospheric Radiation, Williamsburg, Virginia, pp. 141-144, May 13-16, 1986.
- [9] F. X. Kneizys, E. P. Shettle, L. W. Abreu, J. H. Chetwynd, G. P. Anderson, W. O. Gallery, J. E. A. Shelby, and S. A. Clough, *User's Guide to LOW-TRAN7*, AFGL-TR-88-0177, Air Force Geophysics Laboratory, Hanscom AFB, Massachusetts, 1988.

- [10] P. Beckmann and A. Spizzichino, *The Scattering of Electromagnetic Waves From Rough Surfaces*, Elmsford, New York: Pergamon Press, 1963.
- [11] J. Nelson, T. Mast, and S. Fabers, eds., *The Design of the Keck Observatory and Telescope*, Keck Observatory Report No. 90, Lawrence Berkeley Laboratory, University of California, Berkeley, California, January 1985.

Table 1. Typical parameter values for an Earth-Saturn optical communications channel

Transmitter characteristics	
Wavelength	532 nm
Laser output power	2 W
Pulsewidth	10 ns
Aperture diameter	0.5 m
Obscuration diameter	0.15 m
Optics efficiency	0.65
Pointing bias error	0.5 μ rad
Pointing jitter	0.5 μ rad
Other parameters	
Receiver aperture diameter	10 m
Receiver obscuration diameter	4.3 m
Earth-Saturn distance	10.5 AU
Bit error rate with coding	10^{-6}
Alphabet size	256
Daytime data rate ^a	106 kb/sec
Nighttime background irradiance	$0.5 \times 10^{-8} \text{ W/m}^2 \cdot \text{sr} \cdot \text{nm}$
Nighttime data rate ^b	300 kb/sec
^a Obtained by using the base value for daytime background irradiance shown in Table 2.	
^b Obtained by using nighttime background irradiance and an Earth-Saturn distance of 9 AU.	

Table 2. Link performance uncertainties in terms of link margin for a typical Earth-Saturn optical communications channel, including best estimate (base) and range of parameter values

Parameter	Base	Favorable	Adverse	Favorable, dB	Adverse, dB
Receiver optics efficiency	0.4	0.7	0.3	4.5	2.2
Filter efficiency	0.4	0.5	0.25	3.6	1.7
Filter bandwidth, Å	0.3	0.25	0.5	3.3	2.1
Atmospheric transmission	0.48	0.55	0.1	3.4	-1.7
Blur diameter, μrad	162	28	184	4.8	0.8
Detector efficiency	0.5	0.55	0.2	3.3	0.3
Daytime stray-light irradiance, ^a $\text{W}/(\text{m}^2 \cdot \text{sr} \cdot \text{nm})$	0.17×10^{-4}	0.1×10^{-6}	0.65×10^{-2}	3.8	0.8
Daytime background irradiance, ^a $\text{W}/(\text{m}^2 \cdot \text{sr} \cdot \text{nm})$	0.17	0.1	0.65	3.8	0.8

^aDaytime background and stray-light irradiance are varied together to obtain favorable and adverse link margins.

Table 3. Blur diameter estimate, μrad

Parameter	Base	Favorable	Adverse
Mirror quality	90	23	90
Gravity sag	100	10	100
Piston, tilt, decenter due to thermal and mechanical force loading	90	10	120
Atmospheric seeing	5	5	25
Dome seeing	5	5	25
Total RMS blur diameter	162	28	184

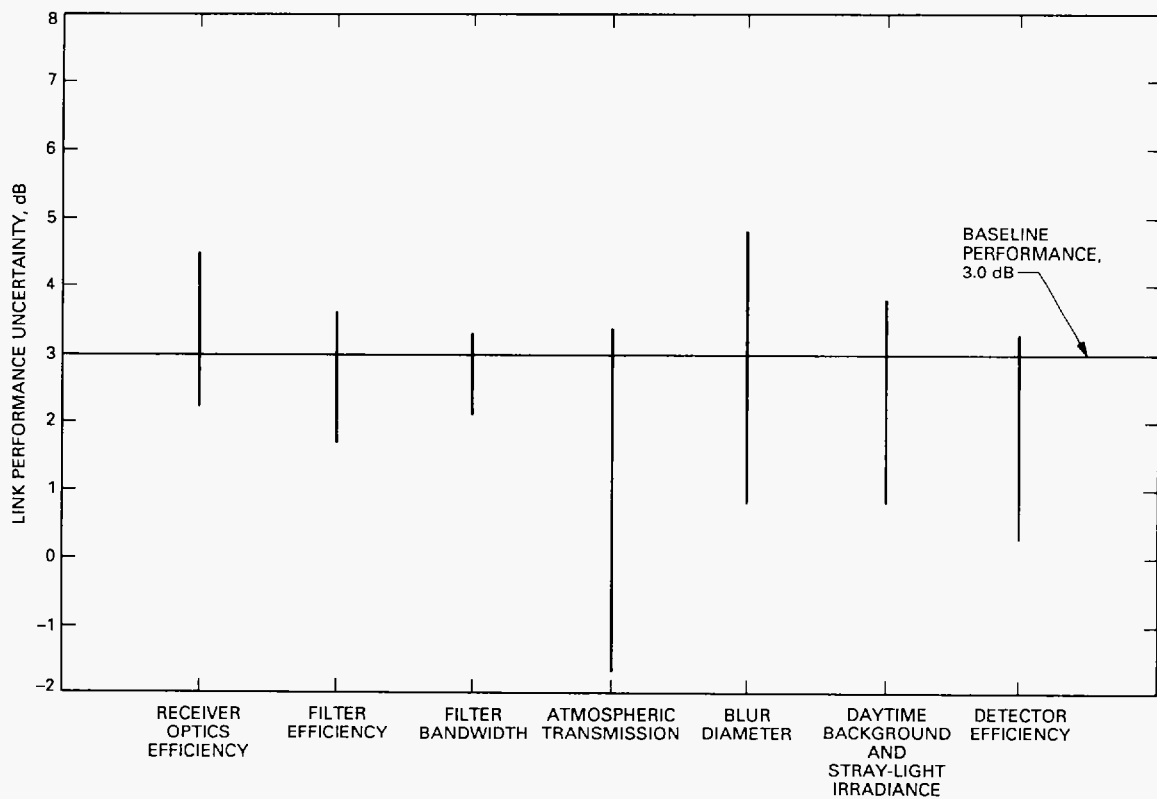


Fig. 1. Link performance uncertainty chart for a typical Earth-Saturn optical communications channel.

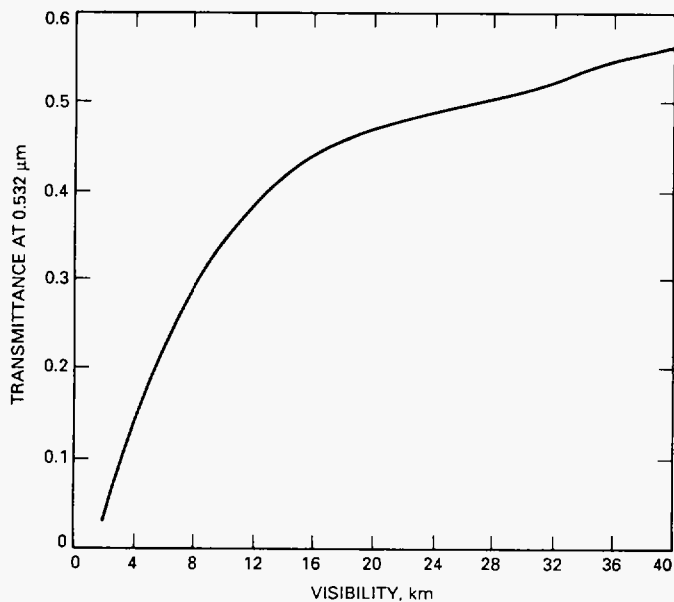


Fig. 2. Atmospheric transmittance versus meteorological visibility assuming a slant path of 45 deg, 1976 U.S. Standard Atmosphere, standard cirrus clouds, and a ground altitude of 2 km.

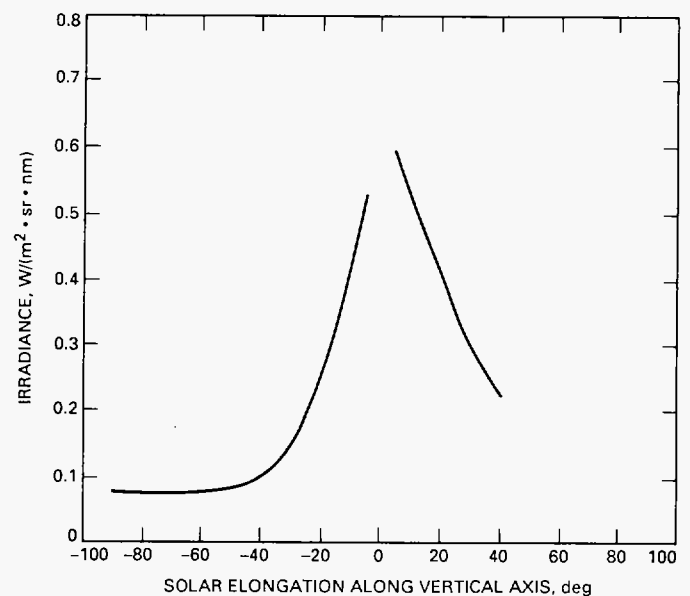


Fig. 3. Solar background irradiance versus solar elongation at 0.532 μm when scanning the sky along the elevation (vertical) axis and assuming a 45-deg solar zenith, 1976 U.S. Standard Atmosphere, standard cirrus clouds, and a ground altitude of 2 km.

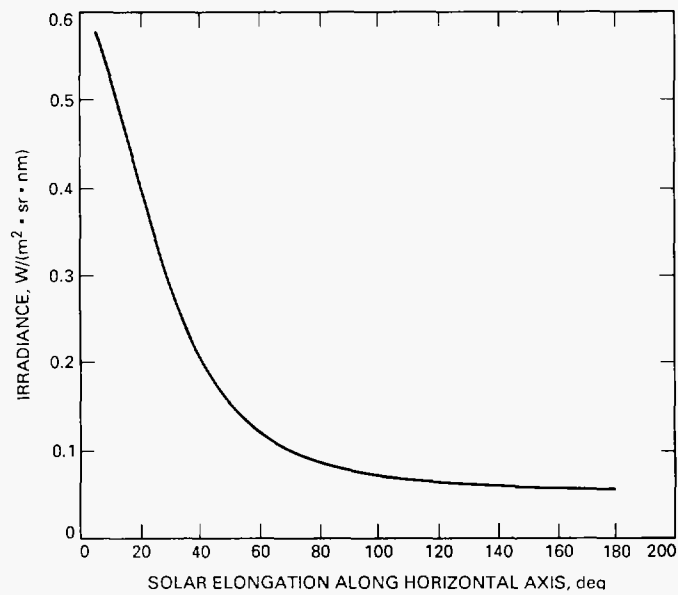


Fig. 4. Solar background irradiance versus solar elongation at $0.532 \mu\text{m}$ when scanning the sky along the azimuth (horizontal) axis and making the same assumptions as in Figs. 2 and 3.

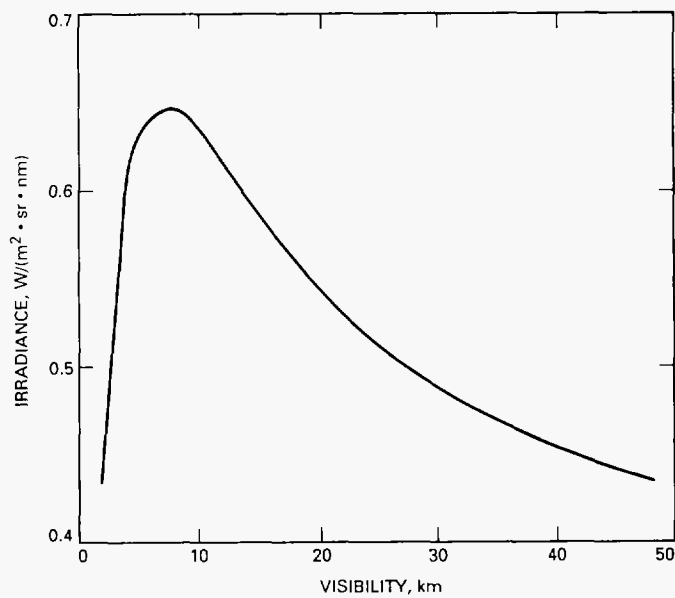


Fig. 5. Solar background irradiance as a function of meteorological visibility at $0.532 \mu\text{m}$ for a fixed solar elongation of 10 deg, with the same assumptions as in Fig. 3.